Angewandte Chemie
Eine Zeitschrift der Gesellschaft Deutscher Chemiker

Supporting Information

Dissipative Control over the Toehold-Mediated DNA Strand Displacement Reaction

E. Del Grosso, P. Irmisch, S. Gentile, L. J. Prins, R. Seidel, F. Ricci**

Supporting Information

Chemicals

Reagent-grade chemicals (NaCl, Tris(2-carboxyethyl)phosphine hydrochloride, 1,4-Dithiothreitol, $MgCl_2$, Na_2HPO_4, Trizma hydrochloride) were purchased from Sigma-Aldrich (St Louis, Missouri) and used without further purifications.

Oligonucleotides

HPLC purified DNA - oligonucleotides and modified with Quasar 570 dye (Q570) and a quencher (Black Hole Quencher 2, BHQ-2) were purchased from Biosearch Technologies (Risskov, Denmark) and from Metabion International AG (Planegg, Germany) and employed without further purification.

Oligonucleotide sequences

The following DNA and RNA oligonucleotides modified and non-modified were used. All oligonucleotides were suspended to a final concentration of 100 μM in phosphate buffer 50 mM, pH 7 and stored at -20°C.

System 1: Enzymatically-driven dissipative strand displacement reaction. An RNA fuel strand is used here as the fuel and the RNase H as the fuel-consuming unit (Figures 2,3):

Output: 5'-(Quasar570)-ATA GAT CCT GAT AGC GAG AC-3'

Target: 5'-**TTG CTA G**GT CTC GCT ATC AGG ATC TAT-(BHQ2)-3'

RNA fuel toehold 3-nt: 5'- AUA GAU CCU GAU AGC GAG AC**C UA** – 3'

RNA fuel_toehold 4-nt: 5'- AUA GAU CCU GAU AGC GAG AC**C UAG** – 3'

RNA fuel_toehold 5-nt: 5'- AUA GAU CCU GAU AGC GAG AC**C UAG C** – 3'

RNA fuel_toehold 6-nt: 5'- AUA GAU CCU GAU AGC GAG AC**C UAG CA** – 3'

RNA fuel_toehold 7-nt: 5'- AUA GAU CCU GAU AGC GAG AC**C UAG CAA** – 3'

The above sequences are the DNA/RNA strands for the enzymatically-driven dissipative strand displacement reaction triggered by an RNA fuel strand. The output and target sequences represent the two complementary strands of the original complex duplex, that have been used conjugated to a fluorophore (Quasar570) and a quencher (BHQ-2). The bold bases in the target strand and in the RNA fuel strands represent the complementary toehold-portion.

System 2: Redox-driven dissipative strand displacement reaction (Figure 4):

Output: 5'-(Quasar570)-ATA GAT CCT GAT AGC GAG AC-3'

Target: 5'-**TTG CTA G**GT CTC GCT ATC AGG ATC TAT-(BHQ2)-3'

Disulfide fuel position 5: 5'-ATA GAT CCT GAT AGC **-S-S-** GAG AC**C TAG C**-3'

The above sequences are the DNA strands for the redox-driven dissipative strand displacement reaction triggered by a disulfide fuel DNA strand. The output and target sequences represent the two complementary strands of the original complex duplex, that have been used conjugated to a fluorophore (Quasar570) and a quencher (BHQ-2). The bold bases in the target strand and in the disulfide DNA strand 10-15 represent the complementary toehold-portion.

The disulfide fuel position 5 is a DNA strand split in two portions, one of 10-nt and the other of 15-nt, and separated by a disulfide bond (S-S).

System 2: Redox-driven dissipative strand displacement reaction (Figure S4):

Disulfide fuel position 6: 5'- ATA GAT CCT GAT AG -S-S- CGA GAC **CTA GC** -3'

Disulfide fuel position 7: 5'- ATA GAT CCT GAT A **-S-S-** GCG AGA C**CT AGC** -3'

The two disulfide fuel position 6 and position 7 are DNA strands split in two portions of different length and separated by a disulfide bond (S-S).

System 3: Transient labelling of DNA-based nanostructures. (Figure 5):

Tile sequences:

S1: 5’-CTC AGT GGA CAG CCG TTC TGG AGC GTT GGA CGA AAC T-3’

S2: 5’- *GTC TG*G TAG AGC ACC ACT GAG *AGG TA*-3’

S3: 5’- TCC AGA ACG GCT GTG GCT AAA CAG TAA CCG AAG CAC CAA CGC-3’

S3_tail: 5’- TCC AGA ACG GCT GTG GCT AAA CAG TAA CCG AAG CAC CAA CGC T**TT TTT TTT TTT GTG AAT ATA AGA TCG AAC G**-3’

S4: 5’-*CAG AC*A GTT TCG TGG TCA TCG *TAC CT*-3’

S5: 5’-CGA TGA CCT GCT TCG GTT ACT GTT TAG CCT GCT CTA C-3’

The above sequences are the DNA strands used to assemble the DNA tiles. The italics bases of S2 and S4 represent the sticky end portions that allow the self-assembly into DNA tubular structures. While the bold bases of the S3_tail strand indicates the tail that allows to address the DNA-tiles.

Sequences for the labelling of the DNA structures:

Target: 5'- TT**G CTA G**GT CTC GCT ATC AGG ATC TAT TTT CGT TCG ATC TTA TAT TCA CA-3’

Q570-conjugated DNA strand: 5’-(Quasar570)-ATA GAT CCT GAT AGC GAG AC-3’

Cy5-conjugated RNA fuel: 5’-(Cy5) - AUA GAU CCU GAU AGC GAG AC**C UAG C** -3’

Cy5-conjugated DNA fuel: 5’-(Cy5) - ATA GAT CCT GAT AGC GAG ACC TAG C -3’

The above sequences are the DNA/RNA strands used for the transient labelling of DNA nanostructures. The target and Q570-conjugated DNA strand sequences represent the two complementary strands of the original complex duplex, that have been used conjugated to a fluorophore (Quasar570). The bold bases in the target and in the Cy5-conjugated RNA fuel strands represent the complementary toehold-portion.

System 4: Self-amplification system. (Figure 6):

Output: 5'-(FAM)- GTG GGA GTT GGA GTA GAG TG -3'

Target: 5'- **TTG CTA G**GT CTC GCT ATC AGG ATC TAT *TCC ACC* ACT CTA CTC CAA CTC CCA C-(OnyxQ)-3'

Incumbent: 5'- GTG GAA TAG ATC CTG ATA GCG AGA C-3'

Capture strand: 5'- GTG GGA GTT GGA GTA GAG T*GG TGG* AAT AGA TCC TGA TAG CGA GAC-3'

RNA fuel_toehold 7-nt: 5'- AUA GAU CCU GAU AGC GAG AC**C UAG CAA** – 3'

DNA fuel_toehold 7-nt: 5'- ATA GAT CCT GAT AGC GAG AC**C TAG CAA** – 3'

The above sequences are the DNA/RNA strands used for the self-amplification circuit under dissipative conditions. The output, target and incumbent sequences represent the original complex of the self-amplification system, where they were conjugated to a fluorophore (FAM) and a quencher (Onyx quencher). The bases shown in bold in the target and RNA/DNA fuel strands represent the complementary toehold-portions. The italics bases in the target and capture strands represent the complementary toehold-portion for the capture strand.

Enzymes

Recombinant RNase-H (from New England BioLabs) was used without further purifications. The RNase-H is an endoribonuclease that specifically hydrolyzes the phosphodiester bonds of RNA, if hybridized to DNA.

Fluorescence measurements and data analysis

Fluorescence measurements (for binding curves and time-course experiments) were obtained using a Cary Eclipse Fluorometer (Varian), with an excitation at 545 nm (± 5 nm) and emission at 565 nm (± 10 nm) (for Quasar570 labelled oligos) and with an excitation at 495 nm (± 5 nm) and emission at 520 nm (± 10 nm) (for FAM labelled oligos). Prior to analysis, the base level (fluorescence of the fully hybridized output-target duplex with maximum quenching) was subtracted from all traces. The measurements of the original strand displacement reaction were performed in 100 mM Tris buffer, 10 mM $MgCl_2$, 150 mM NaCl, pH 8.5, at 45°C, while the measurements of the self-amplification system were performed in 100 mM Tris buffer, 10 mM $MgCl_2$, 150 mM NaCl, pH 8.5, at 37°C

A self-written Python (version 3.7) script was used to analyze the data. The script numerically integrates a set of ordinary differential equations (describing the model reaction scheme) using the “odeint” function and fits the solution to the measured kinetics using a nonlinear least-squares method (“curve_fit”). Both, utilities (“odeint” and “curve_fit”) are part of the SciPy package[1].

Kinetic modelling and curve fitting

General considerations

To describe the experimental results obtained with our systems we employed a minimalistic kinetic model, that uses simplified descriptions of the individual reaction steps.

Specifically, it describes individual strand displacement reactions as irreversible rather than reversible reactions and assumes tight binding of heteroduplexes to RNase H, i.e. saturation of the enzyme kinetics. Such a minimalistic approach, although not entirely formally correct, has the advantage of capturing the key experimental observations without the use of an over-parametrized model that, for the purpose of this work, would be of little value. Generally, the good agreement of our model with the measured data (see below) indicates that despite the made simplifications, the essential reaction steps were correctly described.

Reaction steps consisting of conventional strand displacement reactions (Figure S1 and Figure S4) are assumed to follow second order kinetics according to:

$$AB + C \xrightarrow{k_{\mathrm{displ}}} AC + B, \tag{1}$$

where AB is the initial DNA duplex, consisting of the target strand A and the output strand B. The fuel strand C can displace the output strand B, forming the fuel-target duplex AC. The set of rate equations used to describe the reaction are:

$$\frac{d[AB]}{dt} = \frac{d[C]}{dt} = \quad - k_{\mathrm{displ.}}[AB][C], \tag{2}$$

$$\frac{d[AC]}{dt} = \frac{d[B]}{dt} = \quad + k_{\mathrm{displ.}}[AB][C]. \tag{3}$$

The measured fluorescence signal F was related to concentrations using a linear scaling parameter I as:

$$F = I[B]. \tag{4}$$

Rate model for the enzymatically-driven dissipative strand displacement reaction

Data shown in Figures 2 and 3 and Figure S3 were modelled according to the kinetic scheme shown in Figure S2.

The reaction scheme in Figure S2 starts with a strand displacement step, which follows second order kinetics:

$$AB + C \xrightarrow{k_{\mathrm{displ}}} AC + B, \tag{5}$$

where AB is the output-target duplex and C the RNA fuel strand. Subsequent RNA hetero-duplex cleavage is assumed to be a pseudo-first order reaction:

$$AC \xrightarrow{k_{\mathrm{cut}}} A + R, \tag{6}$$

where the rate constant k_{cut} is assumed to be proportional to the enzyme concentration ([RNase H]). This assumes tight substrate-enzyme interaction (negligible dissociation constant), i.e. an enzyme operating under saturation conditions. Additionally, the rate constant was considered to include enzyme inhibition by the cleaved RNA waste fragments ([R]). Within the Michaelis-Menten scheme, the rate constant for competitive inhibition can be expressed as:

$$k_{\mathrm{cut}} = \frac{k_{\mathrm{cleave}}[RNAse\ H]}{1 + \frac{[R]}{K_{\mathrm{frag}}}}, \tag{7}$$

where K_{frag} is the dissociation constant for binding RNA waste fragments by RNase H. Once the RNA is cleaved, strand A can either rebind a DNA incumbent strand or another RNA invader strand. It is assumed that rebinding is fast for both strands and is occurring with the same rate constant k_{rebind} according to:

$$A + B \xrightarrow{k_{\mathrm{rebind}}} AB, \tag{8}$$

$$A + C \xrightarrow{k_{\mathrm{rebind}}} AC. \tag{9}$$

The set of rate equations used to describe the reaction are:

$$\frac{d[AB]}{dt} = -k_{\mathrm{displ}}[AB][C] + k_{\mathrm{rebind}}[A][B], \tag{10}$$

$$\frac{d[C]}{dt} = -k_{\mathrm{displ}}[AB][C] - k_{\mathrm{rebind}}[A][C], \tag{11}$$

$$\frac{d[AC]}{dt} = +k_{\mathrm{displ}}[AB][C] - k_{\mathrm{cut}}[AC] + k_{\mathrm{rebind}}[A][C], \tag{12}$$

$$\frac{d[B]}{dt} = +k_{\mathrm{displ}}[AB][C] - k_{\mathrm{rebind}}[A][B], \tag{13}$$

$$\frac{d[A]}{dt} = \quad + k_{\mathrm{cut}}[AC] - \; k_{\mathrm{rebind}}[A][B] - \; k_{\mathrm{rebind}}[A][C], \tag{14}$$

$$\frac{d[R]}{dt} = \quad + k_{\mathrm{cut}}[AC]. \tag{15}$$

The fluorescence signal F was again related to the concentration of the free incumbent strand using a linear scaling parameter I as:

$$F = I[B]. \tag{16}$$

When fitting the model, we first obtained the displacement rate constant k_{displ} from globally fitting the conventional displacement data using second order kinetics (Figure S2) where k_{displ} was the only kinetic parameter. At the applied concentrations, the rebinding described by k_{rebind} could be assumed to occur on a much faster timescale than the observed signal decay given rate constants for oligonucleotide hybridizations between $10^6 - 10^7 M^{-1}s^{-1}$ for similar conditions.[2,3] We therefore fixed this parameter to $k_{\mathrm{rebind}} = 3.5 \cdot 10^6/Ms$ and verified that the other parameters were practically insensitive to its choice. $k_{\mathrm{cleave}} = (1.21 \pm 0.02) \cdot 10^{-3}/s$ and $K_{\mathrm{frag}} = (0.31 \pm 0.01)\mu\mathrm{M}$ were obtained by globally fitting the transient behavior of the dissipative strand displacement (Figure 3 a/c). Both parameters are uniquely determined, since k_{cleave} sets the time scale of the signal decay and K_{frag} describes the increase of the time constant at high RNA to RNAse-H ratios (Figure 3c) as well as pulse repetitions (Figure 2c).

Rate model for the redox-driven dissipative strand displacement reaction

Data shown in Figure 4 and Figure S6 and Figure S7 were modelled according to the kinetic scheme shown in Figure S5.

The reaction scheme in Figure S5 starts with a strand displacement step, which follows second order kinetics given by:

$$AB + C \xrightarrow{k_{\mathrm{displ.}}} AC + B. \tag{17}$$

Here, the disulfide fuel DNA strand (C) can be cleaved before the reaction as well as after the displacement reaction, resulting in free and target bound cleaved invader C* according to:

$$C \xrightarrow{k_C} C^*, \tag{18}$$

$$AC \xrightarrow{k_C} AC^*. \tag{19}$$

The cleaved disulfide strand then dissociates from the target, with the rate constant k_{diss}:

$$AC^* \xrightarrow{k_{\mathrm{diss}}} A + C^*, \tag{20}$$

which then can bind the incumbent B with rate constant k_{rebind} to form the original complex duplex:

$$A + B \xrightarrow{k_{\mathrm{rebind}}} AB. \tag{21}$$

Additionally, reverse invasion of the cleaved invader parts was considered to occur as a single second order step:

$$AB + C^* \xrightarrow{k_{\mathrm{rev}}} AC^* + B. \tag{22}$$

This reaction scheme was described by the following set of rate equations:

$$\frac{d[AB]}{dt} = -k_{\mathrm{displ.}}[AB][C] + k_{\mathrm{rebind}}[A][B] - k_{\mathrm{rev}}[AB][C^*], \tag{23}$$

$$\frac{d[C]}{dt} = -k_{\mathrm{displ.}}[AB][C] - k_{\mathrm{C}}[C], \tag{24}$$

$$\frac{d[B]}{dt} = +k_{\mathrm{displ.}}[AB][C] - k_{\mathrm{rebind}}[A][B] + k_{\mathrm{rev}}[AB][C^*], \tag{25}$$

$$\frac{d[C^*]}{dt} = +k_{\mathrm{C}}[C] + k_{\mathrm{diss}}[AC^*] - k_{\mathrm{rev}}[AB][C^*], \tag{26}$$

$$\frac{d[AC]}{dt} = +k_{\mathrm{displ.}}[AB][C] - k_{\mathrm{C}}[AC], \tag{27}$$

$$\frac{d[AC^*]}{dt} = +k_{\mathrm{C}}[AC] - k_{\mathrm{diss}}[AC^*] + k_{\mathrm{rev}}[AB][C^*], \tag{28}$$

$$\frac{d[A]}{dt} = +k_{\mathrm{diss}}[AC^*] - k_{\mathrm{rebind}}[A][B]. \tag{29}$$

The fluorescence signal F was related to the concentration of the free signalling strand [B], using a linear scaling parameter I:

$$F = I[B]. \tag{30}$$

When fitting the model, we first obtained the displacement rate constant k_{displ} from globally fitting the conventional displacement data using second order kinetics (Figure S4) where k_{displ} was the only kinetic parameter. Rebinding was again assumed to occur on a much faster timescale compared to the observed signal decay such that the corresponding rate constant was fxed to $k_{\mathrm{rebind}} = 3.5 \cdot 10^6/Ms$ (see above).[2,3] The rate constants k_{C}, k_{diss} and k_{rev} were obtained by globally fitting the transient behavior of the dissipative strand displacement (Figures 4 and S7). The three rate constants are rather uniquely determined since k_{C} sets the time at which the signal maxima are obtained (since it also cleaves free fuel in solution). The rate constants k_{diss} and k_{rev} set the time scale of the signal decays as well as the signal amplitude in equilibrium. Despite some correlation between k_{diss} and k_{rev}, less parameterized models failed to describe the different characteristics of the observed signals. A sensible determination of the three parameters is also supported by the fact that we obtained similar values for k_{C} for all three disulfide positions.

Fluorescence microscopy

DNA-based nanostructures were imaged using an Axio Scope A1 ZEISS microscope. The emitted photons were collected by a 100x oil objective and a monochrome CCD camera (Axiocam 503 mono - ZEISS).

All the samples containing DNA nanostructures were imaged at 100 nM tiles concentration in the corresponding experimental condition. A single drop (2.0 µL) of the sample was deposited on a microscope glass slides and covered with a coverslip (Menzel-Glaser; thickness: 0.13 to 0.16 mm; size: 18x18 mm). DNA-based nanostructures were imaged using a Cy3 filter set (EX: 530-550 nm; BS: 565 nm; EM: 575-635) and a Cy5 filter set (EX: 590-650 nm; BS: 660 nm; EM: 670-730). Exposure time was set to 10000 ms. Fluorescence microscopy images were processed using ZEN 2 lite (ZEISS) software.

Microscopy data processing

Fluorescence microscopy images were analyzed using SPIP Software – Scanning Probe Image Processor – by Image Metrology/Digital Surf (www.imagemet.com) to collect average length and count values of DNA nanotubes. Branched structures, aggregates, and structure lengths less than 0.5 µm were removed from the dataset analysis using SPIP threshold parameters.

Fluorescence microscopy measurements

DNA nanostructures were prepared in H_2O/Mg^{2+} (12.5 mM $MgCl_2$) by mixing S1, S2, S4 and S5 tile strands at 5 µM final concentration, while S3 strand and S3_tail (that contains the addressable tail) were used with a concentration of 2.5 µM. DNA-based nanostructures were annealed using a Bio-Rad Mastercycler Gradient thermocycler PCR machine by heating the samples to 90°C, and cooling to 20°C at a constant rate (1°C / 5min).

To prepare the initial Q570-labelled DNA nanostructures, a solution of the annealed nanostructures (250 nM) was mixed with the target strand (250 nM) and the Q570-conjugated DNA strand (250 nM) in 1 × TAE buffer / 12.5 mM $MgCl_2$, 10 mM DTT, pH 8.0 at 25°C. An aliquot of this sample was diluted at 100 nM tiles concentration and imaged. Then, to demonstrate the transient re-labelling of the DNA nanostructures the solution of the initial Q570-labelled structures was incubated with RNase-H (30U/ml) and upon the addition of the RNA/DNA fuel strand (500 nM), an aliquot of the sample was diluted at 100 nM tiles concentration and imaged at 15 and 30 minutes.

References:

[1] P. Virtanen, *et al*. *Nat. Methods*. **2020**, *17*, 261-272.

[2] D. Y. Zhang, E. Winfree. *J. Am. Chem. Soc*. **2009**. *131*, 17303–17314

[3] J. X. Zhang, J. Z. Fang, We Duan, L. R. Wu, A. W. Zhang, N. Dalchau, B. Yordanov, R. Petersen, A. Phillips, D. Y. Zhang. *Nat. Chem*. **2018**. *10*, 91-98.

Fuel strand	$k_{\mathrm{displ.}}$ $(10^2/Ms)$	k_C $(10^{-3}/s)$	k_{diss} $(10^{-3}/s)$	k_{rev} $(1/Ms)$
Position 5	6.3	5.4	0.2	8
Position 6	4.8	5.0	0.4	26
Position 7	15	7.8	0.8	25

Table S1: Set of rate constants for the redox-driven dissipative strand displacement reactions obtained from the fits of experimental data. $k_{\mathrm{displ.}}$ was obtained by fitting conventional displacement data (Figure S4) while all other rate constants where obtained from fitting dissipative displacement data (Figures 4c and S7).

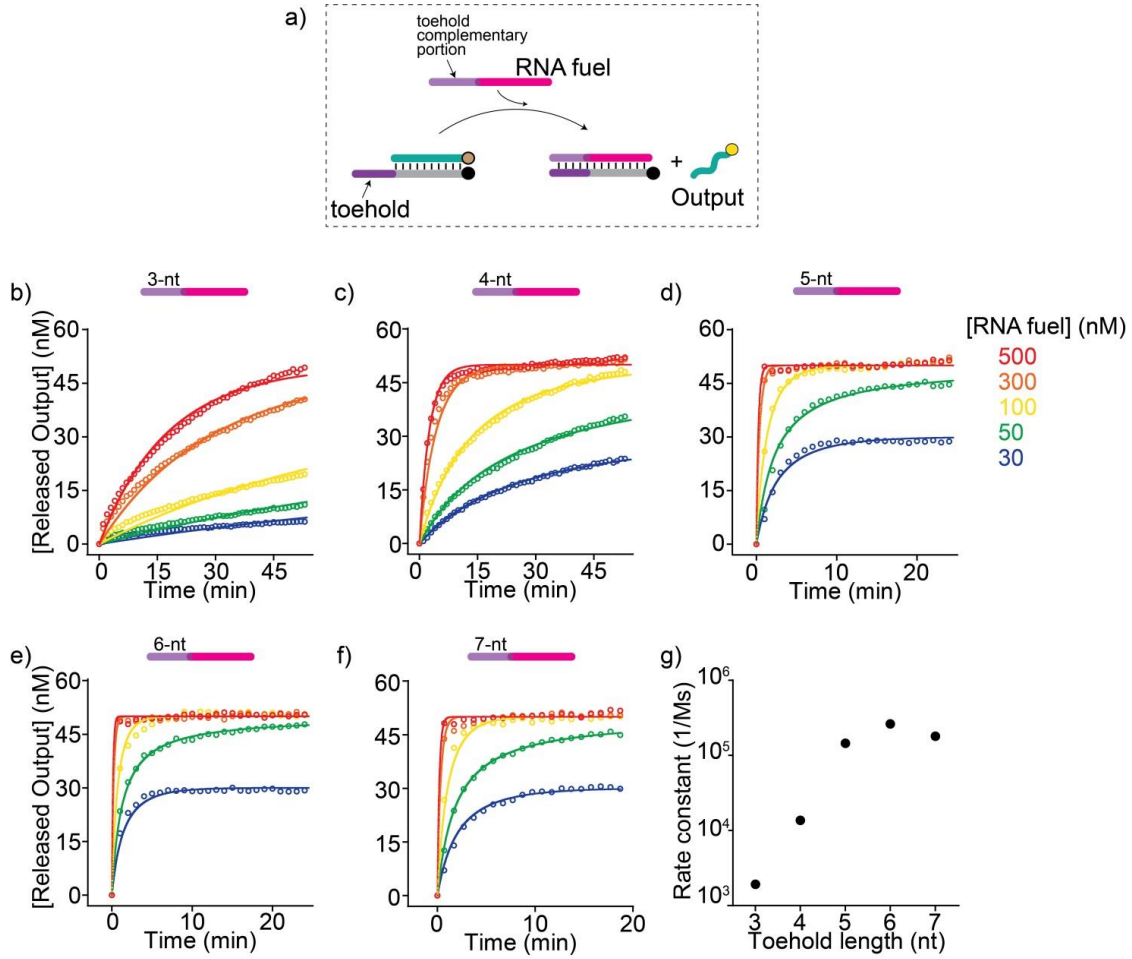

Figure S1. a) Conventional toehold-mediated strand displacement reaction induced by an RNA fuel strand. **b-f)** Strand displacement was measured for a series of RNA fuel strands that shared the same 20-nt invading domains but differed in the length of the toehold part from 3 to 7 nts. Upon addition of the RNA fuel a significant signal increase was observed, indicating the release of the output strand from the initial output-target duplex (50 nM). Solid lines in each plot represent a global fit to the data for all RNA fuel strand concentrations yielding a single second order rate constant for each toehold length. The scaling parameter was fitted individually for each trace. **g)** Obtained second order rates constants for the strand displacement with an RNA invader depending on the toehold length.

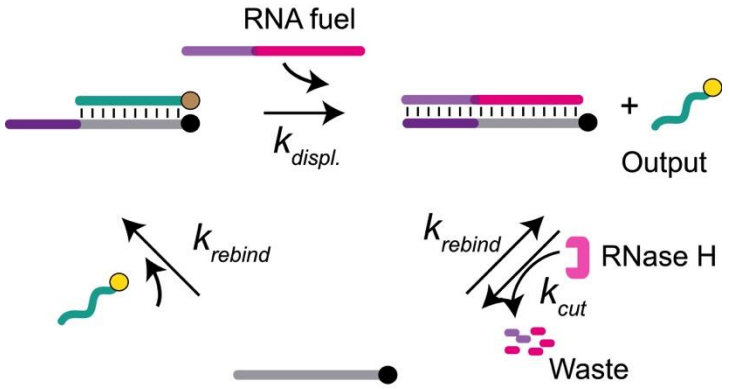

Figure S2. Simple kinetic model for the enzymatically-driven dissipative strand displacement reaction. When fitting the model to experimental data (Figure 3), k_{displ} was taken as fixed value obtained from fitting the conventional displacement reactions in Figure S1 using second order kinetics. k_{rebind} was fixed to the value of $3.5 \cdot 10^{6}/Ms$.[2,3] Global fitting of the transient signal of the dissipative strand displacement (Figure 3 a,c) provided the rate constant for RNA cleavage $k_{\mathrm{cleave}} = (1.21 \pm 0.02) \cdot 10^{-3}/s$ and the dissociation constant for RNase H inhibition by RNA waste fragments $K_{\mathrm{frag}} = (0.31 \pm 0.01)\mu\mathrm{M}$.

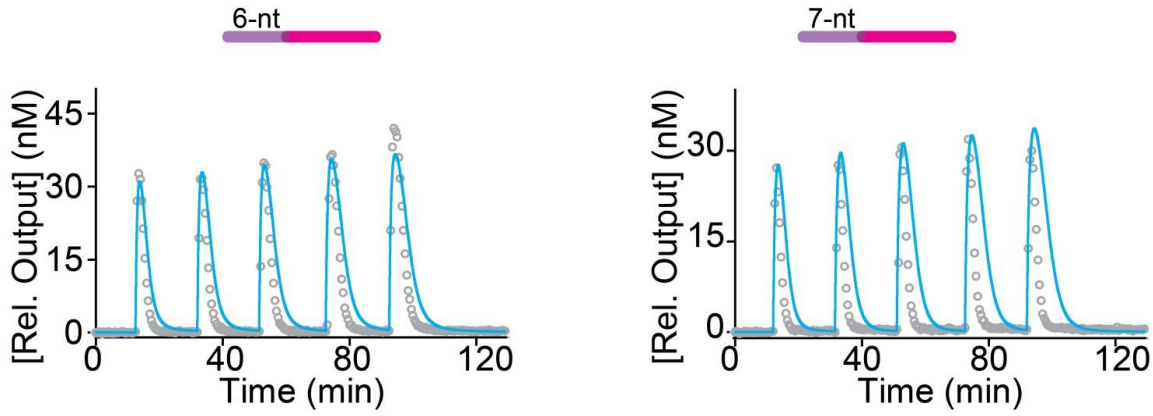

Figure S3. Time trajectories of multiple load/release cycles of the output strand after sequential addition of a fixed concentration of the RNA fuel strands (100 nM) with either a 6 nt (left) or a 7 nt (right) toehold. The solution contained fixed concentrations (50 nM) of the preformed output-target duplex and RNase H (15 U/mL). Solid lines represent the predictions of the kinetic model for the enzymatically-driven dissipative strand displacement reaction (Figure S2) using the second order rate constant obtained for the respective toehold length (Figure S1).

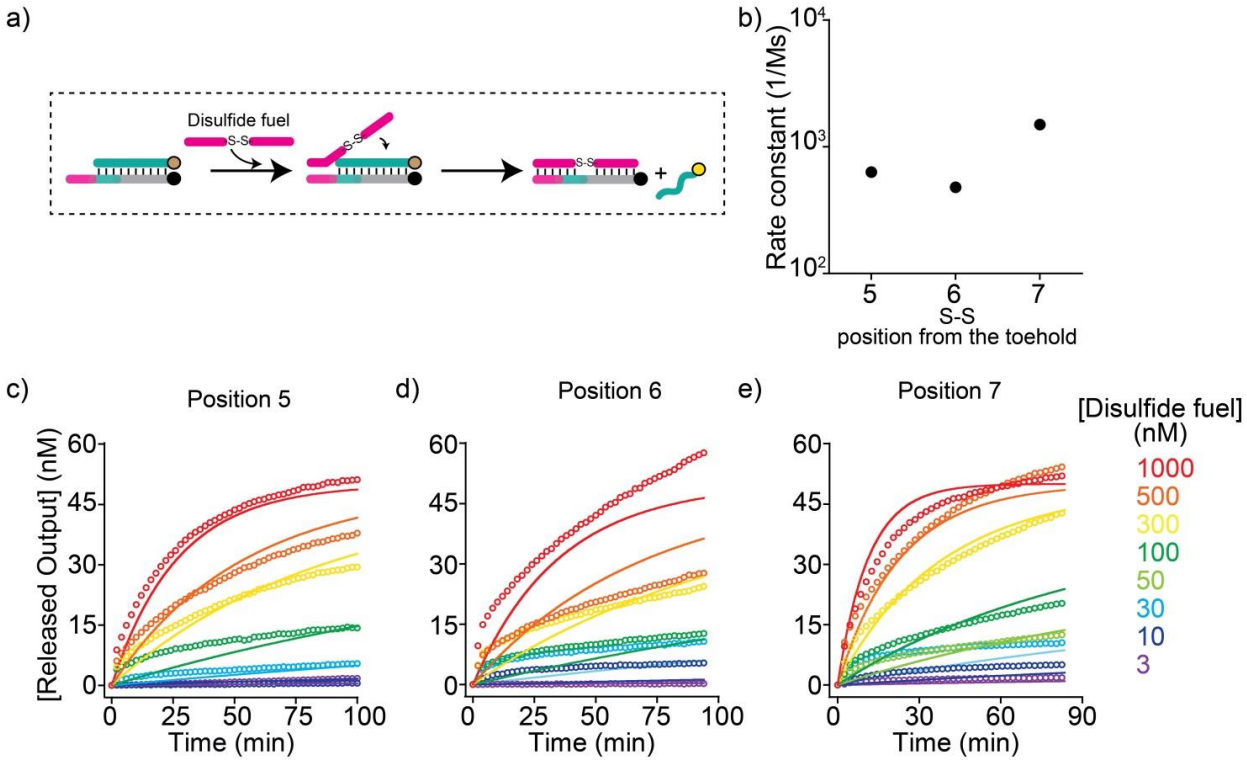

Figure S4. a) Conventional toehold-mediated strand displacement reaction induced by a disulfide fuel DNA strand. **b-e)** Strand displacement was measured for a series of disulfide fuel DNA strands with the same total length, but varying positions of the disulfide bond (5nt, 6nt and 7nt from the toehold end). Upon addition of the disulfide DNA fuel a significant signal increase was observed, indicating the release of the output strand from the initial output-target duplex (50 nM). Solid lines in each plot represent a global fit for all disulfide fuel strand concentrations. The global fit provided for each position one intensity scaling parameter and a second order rate constant. **b)** Obtained second order rate constants of the displacement reaction as function of the disulfide bond position.

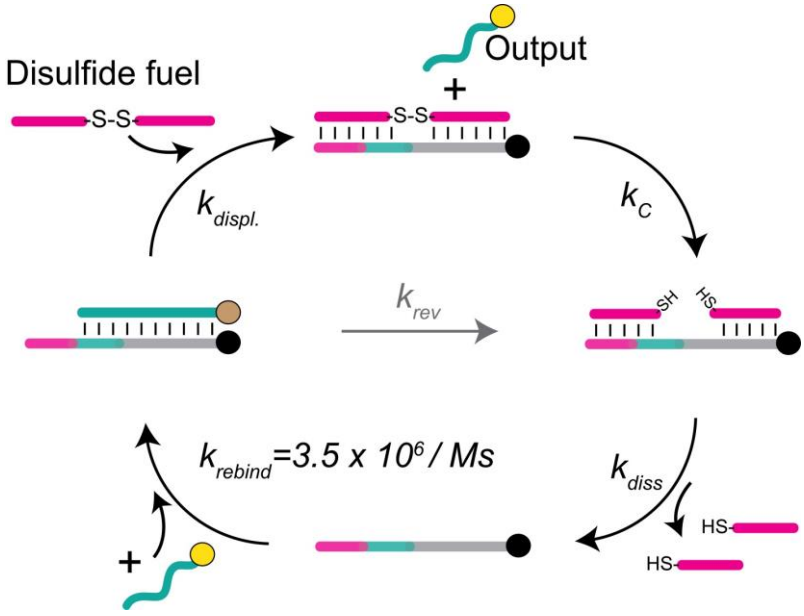

Figure S5. Kinetic model for the redox-driven dissipative strand displacement reaction. When fitting the model to experimental data (Figures 4 and S7), k_{displ} was taken as fixed value obtained from fitting the conventional displacement reactions in Figure S4. Best fit parameters from fitting the model to experimental data for the different disulfide fuels are listed in Table S1.

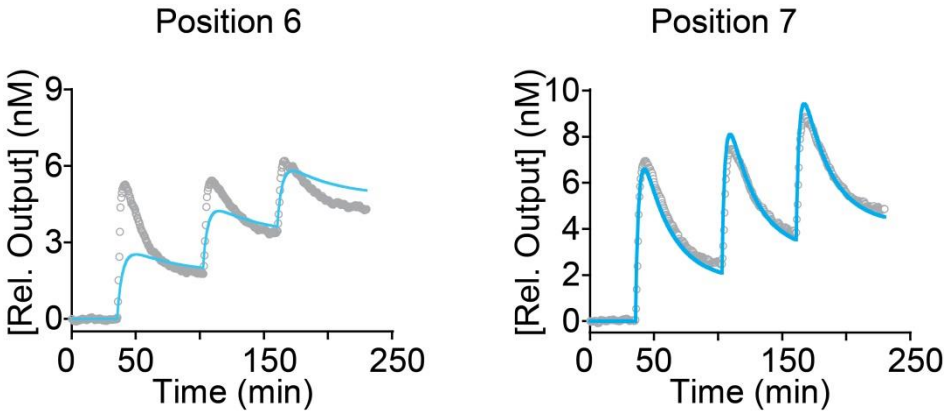

Figure S6. Time trajectories of multiple load/release cycles of the output strand after sequential addition of a fixed concentration of the disulfide DNA fuel strand (100 nM) with the disulfide bond placed either at position 6 (left) or 7 (right). The solution contained fixed concentrations of preformed output-target complex (100nM) and reducing agent (TCEP 1mM). Solid lines are predictions of the kinetic model for the redox-driven dissipative strand displacement reaction using the rate constants provided in Table S1. To compare the model predictions to fluorescence trajectories, a scaling parameter was fitted for each trajectory.

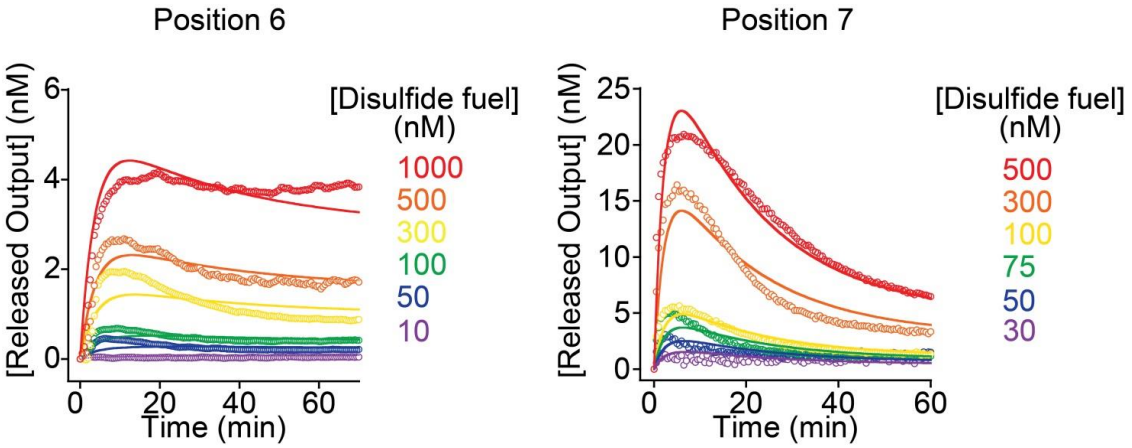

Figure S7. Measured time trajectories of redox-driven dissipative strand displacement reactions at different concentrations of the disulfide fuel in which the disulfide bond was either located 6nt (left) or 7nt (right) from the toehold end. All reactions contained 50 nM preformed output-target duplex and 1mM TCEP as reducing agent. Solid lines in each plot represent a global fit to the transient displacement kinetics for all fuel concentrations. For each trajectory an individual scaling parameter was fitted. Best fit parameters providing the rate constants k_{C}, k_{diss} and k_{rev} for each system are given in Table S1.

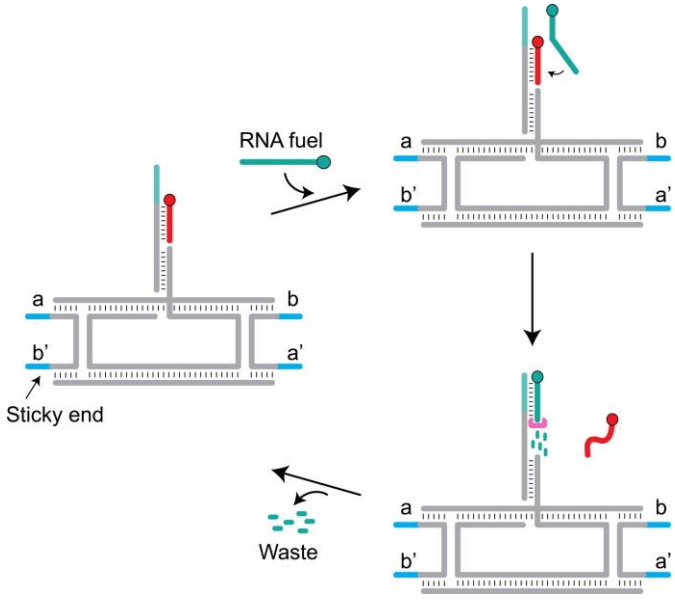

Figure S8. Scheme showing the tile design and the transient labelling reaction of a single tile. Each tile consisted of five DNA strands. The ssDNA overhangs a, b, a' and b' supported the assembly of the DNA nanotubes. A ssDNA overhang supported the attachment of the target-output duplex by hybridization. The output duplex was conjugated with a Quasar570- fluorophore (red). After addition of the Cy5-labelled RNA fuel strand (green), the output strand including Q570 label was displaced by strand displacement reaction, such that the tile became labelled with Cy5. In the presence of RNase-H, the relabelling was transient because the Cy5-labelled RNA strand became degraded over time such that the original Quasar570-conjugated DNA strand could bind again.

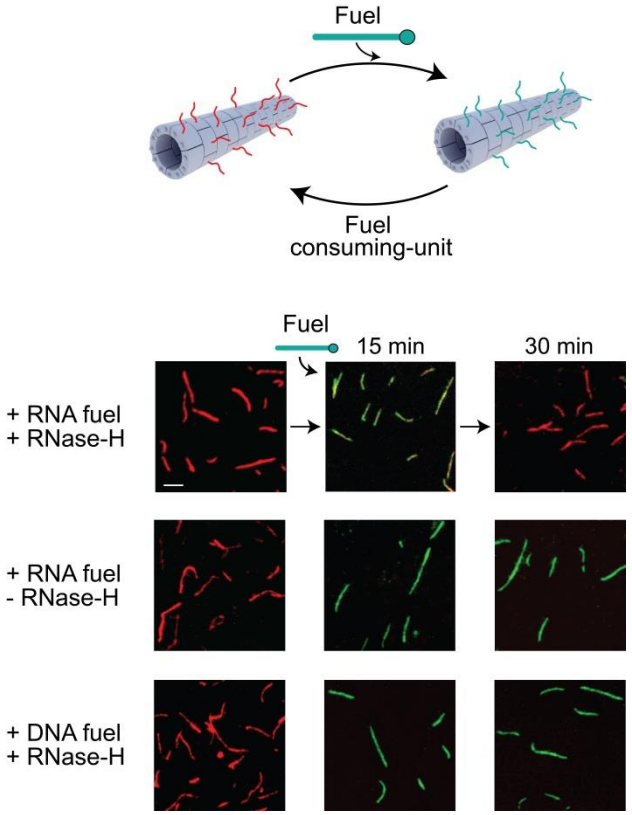

Figure S9. Fluorescence microscopy images showing the transient and permanent relabelling of DNA nanostructures. We started from DNA nanostructures labelled with a Quasar570-conjugated output strand (red in the figure). Upon the addition of a Cy5-conjugated RNA fuel strand (green in the figure), the tubes became labeled by the Cy5-RNA through a strand displacement reaction. In the presence of RNase-H, the relabelling was only transient due to RNA degradation and rebinding of the DNA output strand (microscope images on top), such that the DNA nanostructures will appear red again over time. In contrast, in the absence of the RNase-H or when using a Cy5-conjugated DNA fuel strand, the displacement of the Q570 output strand and the relabelling of the structures with Cy5-labeled strands was permanent such that the nanostructures remained green over time.

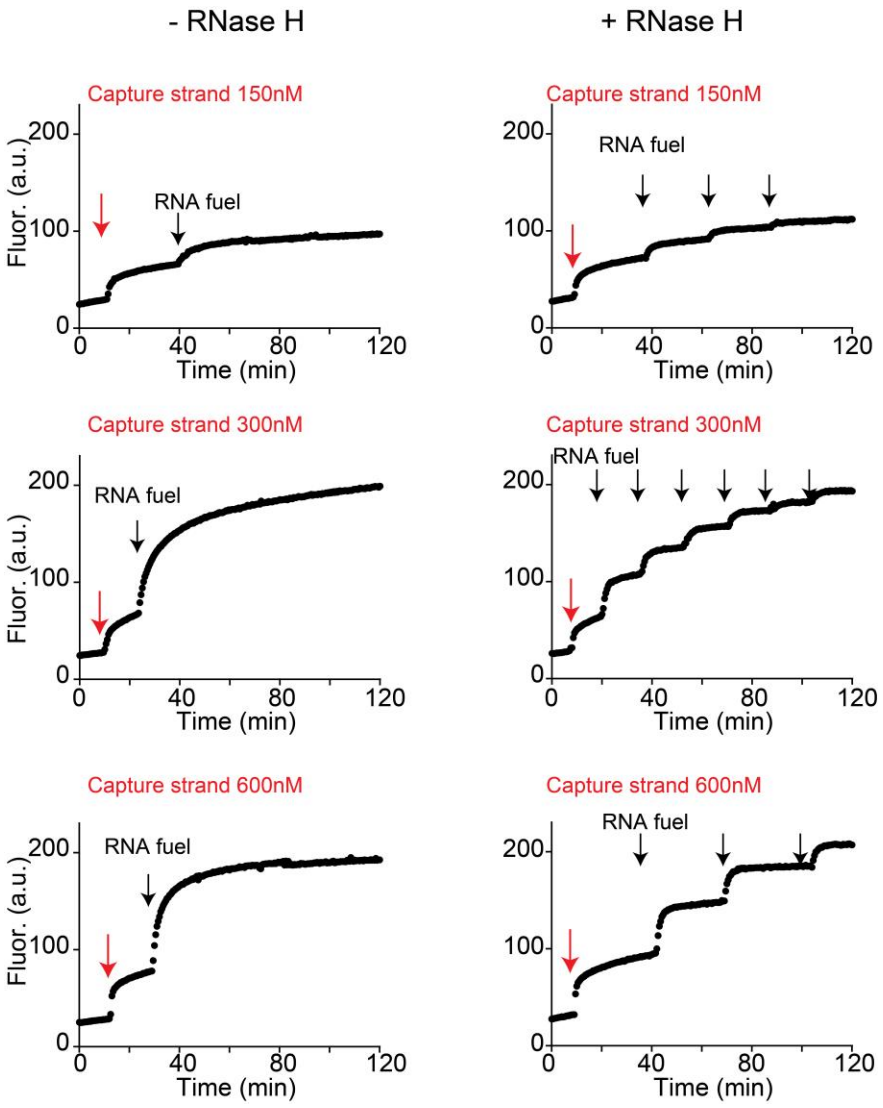

Figure S10. Temporal control of a self-amplification circuit using dissipative strand displacement. By changing the concentration of the capture strand we can modulate the system dynamics. At reduced capture strand concentrations, the turnover of the amplification is reduced in the presence (right) and absence (left) of RNase H. At increased capture strand concentrations, the turnover of the amplification is increased in the presence of RNase H. This can be attributed to the dissociation of the RNA/DNA heteroduplex before the RNA is cleaved. Time trajectory of the output strand release upon addition of different concentrations of capture strands (150, top; 300 nM, center; 600 nM, bottom, indicated by red arrows) and different additions of RNA fuel strand (50nM, indicated by black arrows). The amplification system in the solution contained 300 nM of target, incumbent and output.